

2.5D Forward Solver To Model Scattering Of Long Dielectric Cylinders In An Active Millimeter Wave Imaging System

S. Van den Bulcke and A. Franchois

Department of Information Technology
Ghent University, Sint-Pietersnieuwstraat 41, B-9000 Ghent, Belgium
sara.vandenbulcke@ugent.be, ann.franchois@ugent.be

Abstract: This paper presents an exact forward solver to calculate the three-dimensional (3D) electromagnetic scattered field of an infinitely long dielectric cylinder with an arbitrary, inhomogeneous cross-section, which is illuminated with a given 3D time-harmonic incident field. A 2.5D configuration is adopted. This is a suitable approach for quasi 2D objects and it leads to a significant reduction in computational cost when the cross-sectional dimensions are several to many wavelengths in size. The 3D scattered field contributions in a space - spatial frequency domain are calculated by discretizing a contrast source integral equation with the Method of Moments. The resulting linear system is solved iteratively with a stabilized biconjugate gradient Fast Fourier Transform method. The accuracy and efficiency of the solver are demonstrated by comparison to 2D-TE analytic solutions and to results obtained by a full 3D solver. This forward solver is used to study the scattering behavior in a free-space active millimeter-wave imaging system, which is currently being developed at the Vrije Universiteit Brussel.

Keywords: Millimeter wave scattering, long dielectric cylinders, contrast source integral equation, 2.5D forward solver

1. Introduction

A free-space active millimeter-wave (mm-wave) imaging system is being developed at the Vrije Universiteit Brussel, in order to study the performance of various imaging modes for applications in indoor security and non-destructive testing [1], [2], [3]. The system presently consists of a mm-wave vector network analyzer operating in the 75 to 300 GHz range, which measures the S-parameters in amplitude and phase with a dynamic range of more than 80 dB. At the transmitting side a horn antenna emits an incident Gaussian beam, which is focused by a lens at the object location. At the receiving side the scattered field is focused by a lens for image formation at a receiving horn antenna. The total distance between transmitting and receiving sides typically is 75 cm.

In the development of this active millimeter wave imaging system, it is important to know the scattering behavior of the illuminated objects. The dimensions of the objects (hundreds of mm) are typically much larger than the wavelength (1-10 mm, corresponding to frequencies in the range 30 to 300 GHz), such that a full 3D forward solution is hardly feasible in terms of memory use and computation time. Therefore, only quasi two-dimensional (2D) objects are considered here, but the fields are three-dimensional (3D) such that this so-called 2.5D approach still allows to accurately study the scattering in a mm-wave imaging system.

This paper presents an exact forward solver to calculate the 3D electromagnetic scattered field of an infinitely long dielectric cylinder with an inhomogeneous cross-section. This 2.5D problem is expanded in a number of 2D problems using a spatial Fourier transform with respect to the coordinate z along the cylinder's

axis. Each 2D problem corresponds to one Fourier spectral parameter. The different 2D solutions are then recombined to one 2.5D solution using an inverse Fourier Transform with respect to the same coordinate z . A similar approach is also used in [4]. In case of a pure 2D illumination, the incident field is typically a plane wave, a line source or a Gaussian beam, which has a propagation vector \mathbf{k} in the cross-sectional plane. In the 2.5D case, the incident field is for example a plane wave or a Gaussian beam with oblique incidence. These incident fields have few spectral components, limiting the total number of 2D problems to be solved. Each 2D problem is formulated as a contrast source integral equation (CSIE) and discretized with the Method of Moments (MoM). The resulting linear system is solved iteratively with a stabilized biconjugate gradient Fast Fourier Transform algorithm (BiCGSTAB-FFT) [5], [6]. This method is an efficient and accurate scheme for solving scattering problems [7].

The formulation of the scattering problem is given in section 2. Two types of validations are presented. In section 3., scattered field solutions obtained with the 2.5D solver for pure 2D illuminations are compared to 2D-TE analytic solutions. Solutions for oblique plane wave incidences are compared to full 3D solutions in section 4.

2. Theory and Formulation

The problem is formulated in the frequency domain and the time dependence $\exp(-i\omega t)$ is omitted. Consider a 2D inhomogeneous dielectric object embedded in free space with complex permittivity

$$\epsilon(\mathbf{r}) = \epsilon_r(\mathbf{r})\epsilon_0 = \epsilon'(\mathbf{r}) + i\epsilon''(\mathbf{r}), \quad (1)$$

with $\epsilon'(\mathbf{r})$ and $\epsilon''(\mathbf{r})$ representing the real and imaginary part of $\epsilon(\mathbf{r})$ and $\mathbf{r} = (x, y)$ the 2D position vector. The imaginary part of the relative complex permittivity $\epsilon_r(\mathbf{r})$ is given by $\epsilon_r''(\mathbf{r}) = \frac{\sigma(\mathbf{r})}{\omega\epsilon_0}$, with ω the angular frequency, ϵ_0 the permittivity of vacuum and σ the electric conductivity. The 2D object is located in the horizontal xy plane, thus corresponding to an infinite cylinder with axis along the z -direction in a 3D cartesian coordinate system (\mathbf{r}, z) . The object is illuminated with a 3D time-harmonic incident field $\mathbf{E}^i(\mathbf{r}, z) = [E_1^i(\mathbf{r}, z), E_2^i(\mathbf{r}, z), E_3^i(\mathbf{r}, z)]$ and the resulting scattered field is defined as

$$\mathbf{E}^s(\mathbf{r}, z) = \mathbf{E}(\mathbf{r}, z) - \mathbf{E}^i(\mathbf{r}, z), \quad (2)$$

with $\mathbf{E}(\mathbf{r}, z)$ the total field.

The three components of the electric flux density $\mathbf{D}(\mathbf{r}, z) = [D_1(\mathbf{r}, z), D_2(\mathbf{r}, z), D_3(\mathbf{r}, z)]$ are chosen as the unknowns of the scattering problem [7]. The derivation of the contrast source integral equation starts from the Maxwell equations

$$\begin{aligned} \nabla \times \mathbf{E}(\mathbf{r}, z) &= i\omega\mu_0\mathbf{H}(\mathbf{r}, z) \\ \nabla \times \mathbf{H}(\mathbf{r}, z) &= \mathbf{J}^i(\mathbf{r}, z) + \mathbf{J}^s(\mathbf{r}, z) - i\omega\epsilon_0\mathbf{E}(\mathbf{r}, z), \end{aligned} \quad (3)$$

where the contrast source $\mathbf{J}^s(\mathbf{r}, z)$ is defined as $\mathbf{J}^s(\mathbf{r}, z) = -i\omega\frac{[\epsilon(\mathbf{r})-\epsilon_0]}{\epsilon(\mathbf{r})}\mathbf{D}(\mathbf{r}, z) = -i\omega\chi(\mathbf{r})\mathbf{D}(\mathbf{r}, z)$, where the normalized permittivity contrast is given by $\chi(\mathbf{r}) = \frac{[\epsilon(\mathbf{r})-\epsilon_0]}{\epsilon(\mathbf{r})}$ and $\nabla = (\partial_x, \partial_y, \partial_z)$.

The 2.5D scattering problem is expanded in a number of 2D problems using a spatial Fourier transform with respect to the coordinate z . The forward spatial Fourier transform is defined as $\hat{g}(\mathbf{r}, k_z) = \int_{-\infty}^{\infty} g(\mathbf{r}, z)e^{-ik_z z} dz$ and the inverse spatial Fourier transform is given by $g(\mathbf{r}, z) = \frac{1}{2\pi} \int_{-\infty}^{\infty} \hat{g}(\mathbf{r}, k_z)e^{ik_z z} dk_z$. Using (2) and applying the Fourier transform on (3), the scattered fields thus satisfy the equations:

$$\begin{aligned} \widehat{\nabla} \times \widehat{\mathbf{E}}^s(\mathbf{r}, k_z) &= i\omega\mu_0\widehat{\mathbf{H}}^s(\mathbf{r}, k_z) \\ \widehat{\nabla} \times \widehat{\mathbf{H}}^s(\mathbf{r}, k_z) &= -i\omega\chi(\mathbf{r})\widehat{\mathbf{D}}(\mathbf{r}, k_z) - i\omega\epsilon_0\widehat{\mathbf{E}}^s(\mathbf{r}, k_z), \end{aligned} \quad (4)$$

in which $\widehat{\nabla} = (\partial_x, \partial_y, ik_z)$. A vector potential $\widehat{\mathbf{A}}^s(\mathbf{r}, k_z)$ satisfies the equation

$$\widehat{\nabla}^2 \widehat{\mathbf{A}}^s(\mathbf{r}, k_z) + k_0^2 \widehat{\mathbf{A}}^s(\mathbf{r}, k_z) = \nabla_{\perp}^2 \widehat{\mathbf{A}}^s(\mathbf{r}, k_z) + (k_0^2 - k_z^2) \widehat{\mathbf{A}}^s(\mathbf{r}, k_z) = -\frac{1}{\epsilon_0} \chi(\mathbf{r}) \widehat{\mathbf{D}}(\mathbf{r}, k_z), \quad (5)$$

with $\nabla_{\perp} = (\partial_x, \partial_y)$ and can thus be written as a convolution over the object domain S :

$$\widehat{\mathbf{A}}^s(\mathbf{r}, k_z) = \frac{1}{\epsilon_0} \int_S \widehat{G}(\mathbf{r}, \mathbf{r}'; k_z) \chi(\mathbf{r}') \widehat{\mathbf{D}}(\mathbf{r}', k_z) d\mathbf{r}', \quad (6)$$

with the Green's function given by $\widehat{G}(\mathbf{r}, \mathbf{r}'; k_z) = \frac{i}{4} H_0^{(1)} \left(\sqrt{k_0^2 - k_z^2} |\mathbf{r} - \mathbf{r}'| \right)$.

The scattered field can be written in function of this vector potential as:

$$\widehat{\mathbf{E}}^s(\mathbf{r}, k_z) = \left(k_0^2 \mathbf{I} + \widehat{\nabla} \widehat{\nabla} \right) \cdot \widehat{\mathbf{A}}^s(\mathbf{r}, k_z). \quad (7)$$

Introduction of (6)-(7) in (2) yields the CSIE for $\mathbf{r} \in S$:

$$\widehat{\mathbf{E}}^i(\mathbf{r}, k_z) = \frac{\widehat{\mathbf{D}}(\mathbf{r}, k_z)}{\epsilon(\mathbf{r})} - \left(k_0^2 \mathbf{I} + \widehat{\nabla} \widehat{\nabla} \right) \cdot \widehat{\mathbf{A}}^s(\mathbf{r}, k_z), \quad (8)$$

in which the x -, y - and z -components of the electric flux density $\widehat{\mathbf{D}}(\mathbf{r}, k_z)$ are the unknowns, and which is solved in an iterative manner.

The object domain S is uniformly discretized in square cells with cell size Δ . In each cell, the complex permittivity is assumed constant and equal to the value at the center point. A Method of Moments with Galerkin weighting is applied to discretize the CSIE, in which the vector potential $\widehat{\mathbf{A}}^s(\mathbf{r}, k_z)$ and the electric field density $\widehat{\mathbf{D}}(\mathbf{r}, k_z)$ are expanded in basis functions. The basis and expansion functions are chosen as products of one-dimensional triangle functions and one-dimensional pulse functions. For the x - (y -) component of the fields we use a one-dimensional triangle function in the x - (y -) direction of support 2Δ and a one-dimensional pulse function in the y - (x -) direction of support Δ . For the z -component triangle functions of support 2Δ are used in both directions. The obtained linear set of equations is solved iteratively with a stabilized biconjugate gradient Fast Fourier Transform method [5], [6].

This forward problem has to be solved for the different values of k_z but only those components in the spectrum with $k_z \in [-k_0, +k_0]$ will contribute to the emitted electromagnetic field. Thus, the resulting value for $\mathbf{E}^s(\mathbf{r}, z)$ is calculated as follows:

$$\begin{aligned} \mathbf{E}^s(\mathbf{r}, z) &= \frac{1}{2\pi} \int_{-k_0}^{+k_0} \widehat{\mathbf{E}}^s(\mathbf{r}, k_z) \exp(jk_z z) dk_z \\ &\approx \frac{\Delta k_z}{2\pi} \sum_{k_z=-k_0}^{k_0} \widehat{\mathbf{E}}^s(\mathbf{r}, k_z) \exp(jk_z z) \end{aligned} \quad (9)$$

with Δk_z the size of the discretization step for k_z .

3. Comparison to 2D-TE analytic solution

To validate the numerical scheme, computations for a pure 2D-TE illumination ($k_z = 0$) are compared to a 2D-TE analytic solution and the normalized root mean square error (NRMSE) is determined:

$$NRMSE = \frac{\sqrt{\sum_{k=1}^N |E_{sim}^s(k) - E_{exact}^s(k)|^2}}{\sqrt{\sum_{k=1}^N |E_{exact}^s(k)|^2}}. \quad (10)$$

The configuration consists of an infinitely long dielectric cylinder with circular cross section with a radius of one free-space wavelength ($\lambda_0 = 1$ mm, $f = 300$ GHz) and a relative permittivity $\epsilon_r = 2$. The incident field $\mathbf{E}^i(\mathbf{r}) = E_1^i(\mathbf{r})\mathbf{u}_x$ is a plane wave propagating in the y -direction and is polarized along the x -direction. The scattered fields $E_1^s(\mathbf{r})$ and $E_2^s(\mathbf{r})$ are calculated in $N = 256$ points on a circle with a radius of $10\lambda_0$. Simulations are performed for different discretizations: 10, 20, 40, 50, 100 and 250 cells per wavelength λ_m inside the cylinder. The BiCGS iterations are stopped when the relative error drops below 10^{-8} .

Fig. 1 shows the amplitude and phase of the x - and y -components of the scattered field on the detector points for a discretization of 10 cells per λ_m . There is a good agreement between the 2.5D solver results (dotted line) and the analytic solution (solid line). Table 1 shows the different parameters of this simulation. The NRMSE for the x - and y -components decreases as $O(1.3\Delta)$.

A comparison between simulation results and analytic solutions for TM polarization yields similar results.

Table 1: Parameters for TE simulations.

cells per λ_m	grid size	# unknowns	# CG iterations	CPU time	NRMSE E_1^s	NRMSE E_2^s
10	64x64	12 288	32	9.99''	0.0361	0.0374
20	128x128	49 152	30	54.06''	0.0138	0.0159
40	256x256	196 608	32	3'50''	0.0066	0.0078
50	512x512	786 432	38	5'35''	0.0036	0.0038
100	1024x1024	3 145 728	43	38'08''	0.0019	0.0022
250	2048x2048	12 582 912	41	3h. 38' 25''	0.0005	0.0005

4. Comparison to a full 3D solver

The 2.5D solver is now compared to a full 3D solver [8]. The scatterer is again a dielectric cylinder with relative permittivity $\epsilon_r = 2$ and a radius equal to one wavelength ($\lambda_0 = 1$ mm, $f = 300$ GHz). With the 2.5D solver, this cylinder is infinitely long, while with the 3D solver, only a finite 3D object can be modelled. The length l of this 3D finite cylinder thus should be chosen long enough, for example $l = 100\lambda_0 = 100$ mm. In both simulations (2.5D and 3D), the scattered fields are calculated for 360 points on a circle with a radius of $2\lambda_0 = 2$ mm which is much closer to the object than in section 3.. The incident field is a TM polarized plane wave with oblique incidence: the propagation vector \mathbf{k} makes an angle of 8 degrees with the xy plane. In the simulations with the 2.5D solver, the BiCGS iterations are stopped when the relative error drops below 10^{-8} , after 60 iterations. With the 3D solver the simulations are stopped when the relative error drops below $10^{-2.5}$, after 360 iterations. The 3D simulation took 16 hours, the 2.5D simulation only 17.65 seconds.

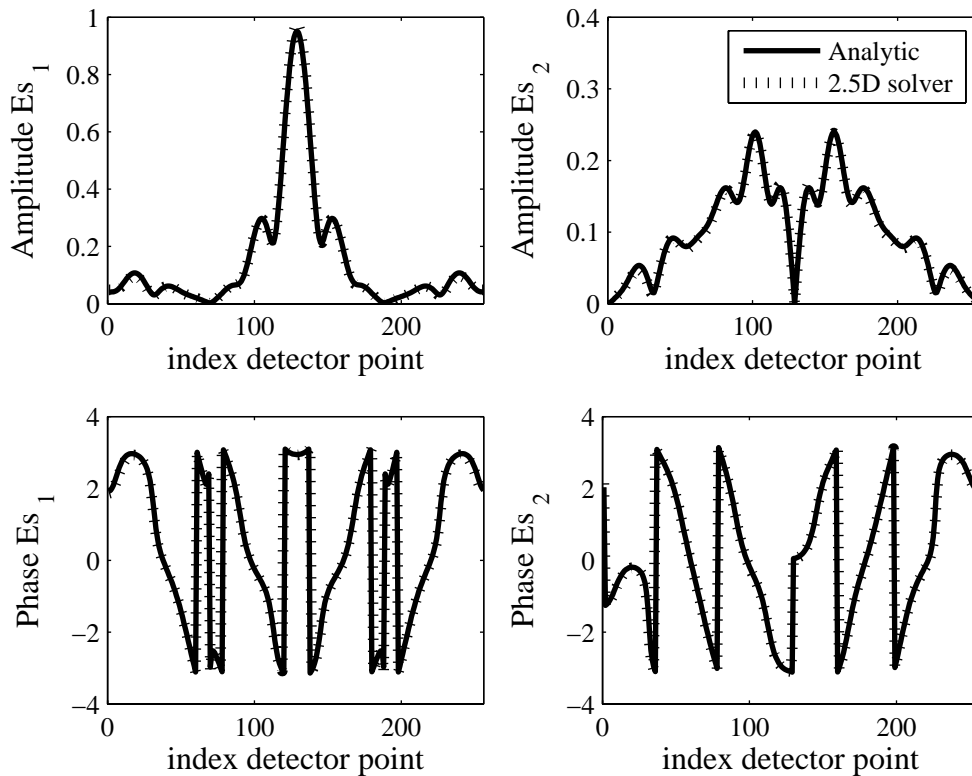


Fig. 1: x (left) and y (right)-component of scattered field; solid line: analytic solution, dotted line: 2.5D solver with 10 cells per λ_m .

The amplitude of the scattered field $|\mathbf{E}_s|$ on the detector is presented in Fig. 2. There is a good agreement between the 2.5D solver (dotted line) and the full 3D solver (solid line). Differences are a consequence of the finite length of the 3D cylinder and the relative low tolerance ($10^{-2.5}$) for the 3D case. Fig. 3 shows the amplitude of the scattered field in a square region of 34 mm x 34 mm centered around the cylinder, where the incident field comes from the left side of the figure.

The 2.5D solver is not only much faster than the 3D solver, it also uses far less unknowns: the 3D problem consists of more than 5 million unknowns and occupies 2.4Gb of memory while the 2.5D problem has only 12 288 unknowns and uses no more than 10 712 Mb of memory. This comparison strongly confirms the choice for a 2.5D solver for simulating long cylindrical objects.

5. Conclusion

A 2.5D BiCGS-FFT solver is developed to compute the interaction between long inhomogeneous dielectric cylinders and incident millimeter waves. A comparison to the analytic solution for the 2D-TE case and to a full 3D solver demonstrates the applicability and accuracy of the proposed method. There is still a discretization error due to the staircase approximation of curved boundaries, which tends to vanish for increasingly finer discretizations. The application of FFT's yields a fast and efficient method for solving scattering problems and the 2.5D configuration strongly reduces the number of unknowns.

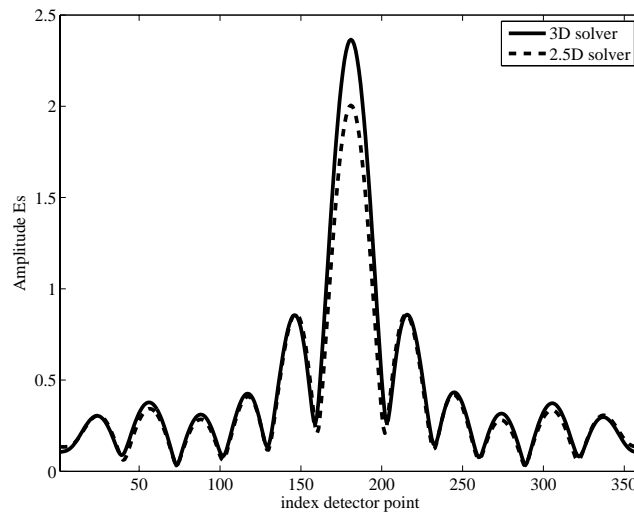


Fig. 2: Amplitude of scattered field on detector.

Acknowledgment

Research funded by a Ph.D. grant of the Institute for the Promotion of Innovation through Science and Technology in Flanders. (IWT-Vlaanderen).

References

- [1] “Visualization of concealed objects using mm wave systems”, a project funded by the Institute for the Promotion of Innovation through Science and Technology in Flanders (IWT-SBO 231.011114).
- [2] L. Volkov and J. Stiens, US patent 6777684: Systems and methods for millimeter and sub-millimeter wave imaging, August 2004.
- [3] I. Ocket, B. Nauwelaers, J. Fostier, L. Meert, F. Olyslager, G. Koers, J. Stiens, R. Vounckx and I. Jäger, “Characterization of speckle/despeckling in active millimeter wave imaging systems using a first order 1.5D model”, *Proc. SPIE Vol. 6194 Millimeter-Wave and Terahertz Photonics*, 2006.
- [4] Aria Abubakar, Peter M. van den Berg, and Tarek M. Habashy, “An integral equation approach for 2.5-dimensional forward and inverse electromagnetic scattering”, *Geophys. J. Int.*, vol. 165, pp. 744-762, 2006.
- [5] X. M. Xu, Q. H. Liu and Z. Q. Zhang, “The stabilized biconjugate gradient fast Fourier transform method for electromagnetic scattering”, *J. Appl. Computat Electromag. Soc.*, vol. 17(1), pp. 97-103, March 2002.
- [6] H. A. van der Vorst, “BI-CGSTAB: A fast and smoothly converging variant of BI-CG for the solution of non symmetric linear systems”, *SIAM Journal on scientific and Statistical Computing*, vol. 13(2), pp. 631-644, 1992.
- [7] Peter Zwamborn and Peter M. van den Berg, “A weak form of the conjugate gradient FFT method for two-dimensional TE scattering problems”, *IEEE Transactions on Microwave Theory and Techniques*, vol. 39, no. 6, pp. 953-960, June 1991.
- [8] P. Lewyllie, A. Franchois, C. Eyraud and J.-M. Geffrin, “Testing a 3D BCGS-FFT solver against experimental data”, *Proceedings of 9th International Conference on Electromagnetics in Advanced Applications*, Torino, Italy, 2005.

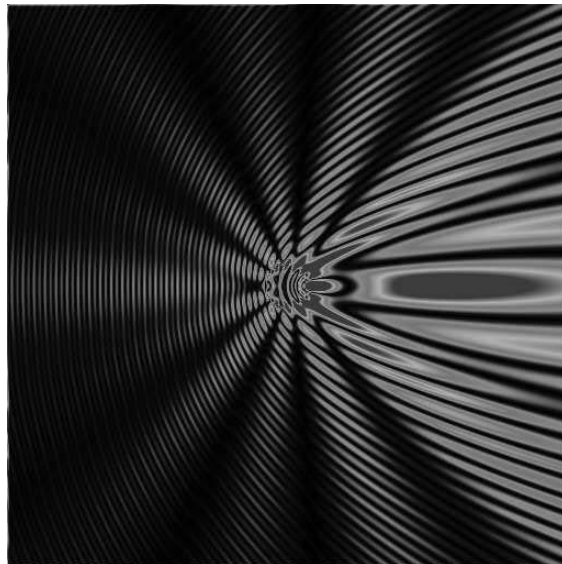


Fig. 3: Amplitude of scattered field on grid points.